Author contributions

BL, WS and HS conceived the idea. HS, QG, CS designed and performed the experiments. JC, CZ, FH, BM and HY supervised the study. HS, QG and PZ performed the experiments and analyzed the data. RHM, JL, XS helped analyze the data and provided valuable advices. HS and CS wrote the manuscript. BL, WS and RHM revised the manuscript.

CD271 Antibody-functionalized Microspheres Capable of Selective Recruitment of Reparative Endogenous Stem Cells for *in situ* Bone Regeneration

Han Sun [a,b,1], Qianping Guo [b,1], Chen Shi [b,c,1], Ross H McWilliam [d], Jianquan Chen [b], Caihong Zhu [b], Fengxuan Han [b], Pinghui Zhou [b,e], Huilin Yang [b], Jinbo Liu [a], Xiaoliang Sun [a], Bin Meng [b,*], Wenmiao Shu [d,*], Bin Li [a,b,f,*]

[a] Department of Articular Orthopaedics, Orthopaedic Institute, The Third Affiliated Hospital, Soochow University, Changzhou, Jiangsu, China;

[b] Department of Orthopaedic Surgery, The First Affiliated Hospital, Soochow University, Suzhou, Jiangsu, China;

[c] Hangzhou R&L Medical Device Co. Ltd., Hangzhou, Zhejiang, China;

[d] Department of Biomedical Engineering, University of Strathclyde, Glasgow, United Kingdom;

[e] Department of Orthopedics, The First Affiliated Hospital of Bengbu Medical College, Bengbu, Anhui, China;

[f] China Orthopaedic Regenerative Medicine Group (CORMed), Hangzhou, Zhejiang, China.

[1] These authors contributed equally to this study.

* Correspondence to: binli@suda.edu.cn (BL); will.shu@strath.ac.uk (WS); mbyang2000@vip.163.com (BM). Tel.: + 86-512-6778-1163 (BL).

Abstract

In the strategy of *in situ* bone regeneration, it used to be difficult to specifically recruit bone marrow mesenchymal stem cells (BM-MSCs) by a single marker. Recently, CD271 has been considered to be one of the most specific markers to isolate BM-MSCs; however, the effectiveness of CD271 antibodies in recruiting BM-MSCs has not been explored yet. In this study, we developed novel CD271 antibody-functionalized chitosan (CS) microspheres with the aid of polydopamine (PDA) coating to recruit endogenous BM-MSCs for *in situ* bone regeneration. The CS microspheres were sequentially modified with PDA and CD271 antibody through dopamine self-polymerization and bioconjugation, respectively. *In vitro* studies showed that the CD271 antibody-functionalized microspheres selectively captured significantly more BM-MSCs from a fluorescently labeled heterotypic cell population than non-functionalized controls. In addition, the PDA coating was critical for supporting stable adhesion and proliferation of the captured BM-MSCs. Effective early recruitment of $CD271^+$ stem cells by the functionalized microspheres at bone defect site of SD rat was observed by the CD271/DAPI immunofluorescence staining, which led to significantly enhanced new bone formation in rat femoral condyle defect over long term. Together, findings from this study have demonstrated, for the first time, that the CD271 antibody-functionalized CS microspheres are promising for *in situ* bone regeneration.

KEYWORDS: Chitosan microspheres, *In situ* regeneration, Polydopamine, Antibody immobilization, Cell recruitment

1. Introduction

In situ bone regeneration, utilizing body's endogenous biological resources and reparative capacity, has been recently developed [11-18]. Instead of seeding cells *in vitro* which may result in loss of boneforming ability on serial passaging in culture [19], biomaterial scaffolds are functionalized with target-specific molecules in order to recruit progenitor stem cells *in vivo*, which will further proliferate and differentiate to regenerate tissues. The new *in situ* bone regeneration approach avoids the complications associated with *ex vivo* cell manipulation and transplantation [16, 20]. Specific recruitment of target progenitor stem cells with adequate quantity at defect sites, therefore, holds the critical key to *in situ* bone regeneration. With outstanding pluripotency, bone marrow mesenchymal stem cells (BM-MSCs), residing in bone marrow, are one of the most efficient seed cells in bone tissue engineering. Unfortunately, the complex cell components and micro-environment within the bone marrow make it challenging to specifically target and recruit BM-MSCs [4, 21]. It has been well studied that BM-MSCs express CD73, CD90, and CD105 [22]. However these markers were also expressed by other types of cells in the bone marrow. Stromal cell-derived factor-1 was reported as an important factor for recruiting BM-MSCs, yet the selectivity was relatively low, resulting in the non-specific recruitment of hemopoietic stem cells which lacked osteogenesis capacity [23]. Other chemoattractant, like bone morphogenetic proteins, was also applied for the recruitment of BM-MSCs, but negative impacts on bone regeneration were reported [24, 25].

In 2002 Quiric et al. have confirmed that CD271 (also called Nerve Growth Factor Receptor (NGFR), Low-affinity Nerve Growth Factor Receptor (LNGFR) or p75 neurotrophin receptor (p75NTR)) antigen is specifically expressed in a group of human BM cells with multi-directional differentiation potential,

and this expression could keep existence during further culture without growth factor stimulation *in vitro* [26]. Subsequently, studies found that $CD271^+$ cells sorted by CD271 antibody exhibited high CFU-F activity and osteogenic differentiation potential [27, 28]. Meanwhile, $CD271^+$ cells displayed high positivity for CD73, CD90, and CD105, while lacking expression of human leukocyte DR and other antigens in the first three passages [27]. These findings indicate that $CD271^+$ cells possess the characteristics of mesenchymal stem cells, which are similar to human BMSCs obtained by traditional adherent method. It is worth noting that sorting based on CD271 antibody hold the least potential of contaminating hematopoietic-lineage cells, which makes CD271 one of the most specific markers to purify hBM-MSCs [30]. Moreover, CD271 antigen also plays an important role in cell migration [31, 32]. Therefore, we hypothesized that CD271 antibody could be an effective factor for specifically recruiting BM-MSCs *in vivo* for *in situ* bone regeneration. Scaffold is an important component of bone repair material system, which bearing the adhesion, proliferation, and differentiation of stem cells. Compared with macroscopical scaffolds, microspheres are small enough for injection therapy via minimally invasive surgical methods [35]. Cell loaded system based on microspheres can provide sufficient surface for cell attachment, and offer direct exchange of materials with surrounding, making it possible for cells to proliferate on the microspheres [36]. Moreover, these particles possess unique properties for drug/growth factor release and surface modification, making them easily to be mixed for more complex system as building blocks [9]. On the other hand, being suitable for cell attachment and polarization is also essential to scaffolds in bone regeneration. In some cases surface modification is necessary to improve these characteristics. Messersmith and his co-workers found that dopamine (DA) can be used to readily modify the surface of materials [40]. In the weak alkaline buffer solution, the DA

can form polydopamine (PDA) by base-triggered oxidation and further deposit on various surface via self-polymerization [41]. The PDA coating can provide the high hydrophilicity and bioactive functional groups to facilitate the cell attachment and expansion on the surface of materials [42].

In this study, we designed and fabricated a novel PDA coated chitosan (CS) micrsopheres functionalized with the CD271 antibody for *in situ* bone regeneration. The functional microspheres held high efficiency in the targeted recruitment of BM-MSCs and was suitable for cell attachment and proliferation, which finally facilitated new bone formation *in vivo*. This work provides valuable information into the design of scaffolds with specific cell targeting and recruitment capacity for *in situ* bone regeneration and the reported biomaterial strategy can be readily applied to engineer and regenerate many other types of tissues.

2. Materials and Methods

2.1 Study design

We fabricated submicron CS microspheres and modified them with PDA. Then, the biotin modified CD271 antibody was grafted onto the surface of microspheres by biotin-SAV pair. The expression of CD271 antigen in various kinds of cells we used was detected by flow cytometry. Subsequently, hBM-MSCs were pre stained and co-cultured with microspheres to detect the ability of microspheres to capture hBM-MSCs. The proliferation of the captured cells on the surface of microspheres was investigated by phalloidin/DAPI staining. Then, the ability of functional microspheres to capture hBM-MSCs from heterotypic cell suspension was further tested. hBM-MSCs and hPBMCs were pre-stained into green and

red respectively and then mixed. After co-culture with the functional microspheres, the capture was judged by observing the fluorescence color of the cells on the surface of the microspheres. Finally, the lateral femoral condyle defect model of SD rat was prepared with microsphere implantation. The early recruitment of cells *in vivo* was observed by taking out the microspheres along with CD271/DAPI immunofluorescent staining, and bone regeneration of long term were tested by micro-CT and tissue section staining.

2.2 Fabrication of CD271-functionalized chitosan microspheres

2.2.1 Fabrication of chitosan (CS) microspheres

Chitosan microspheres were prepared by using high-voltage electrostatic method. Acetic acid (Aladdin, Shanghai, China) was firstly mixed with deionized water to prepare 2% v/v acetic acid solution. Chitosan powder (Aladdin, Shanghai, China) was then dissolved in the acetic acid solution at a concentration of 2% w/v. Afterwards, the chitosan solution was injected into 1.0 M sodium hydroxide solution using a jetting equipment consisting of a high pressure electrostatic generator, a micro-injecting pump (LSP02-1B, Baoding Longer Precision Pump Co., Ltd., China), a 20 ml syringe and a nozzle. The collected chitosan microspheres were repeatedly washed by deionized water, and then were filtered by a 100 μm strainer to sift out smaller microspheres. After being sterilized with 75% ethanol, the prepared microspheres were washed with phosphate buffered saline (PBS) (Hyclone, Logan, USA) solution and stored in the PBS solution at 4 ° C for further use.

2.2.2 Polydopamine (PDA) coating on chitosan microspheres (PDA/CS)

Dopamine hydrochloride (Alfa Aesar, Heysham, UK) was dissolved in 10 mM Tris-HCl solution (pH 8.5) at a concentration of 2 mg/mL. Then the chitosan microspheres were immersed in the dopamine

hydrochloride solution for the deposition of PDA coating. After reacting at room temperature for 12 hours, the microspheres were collected and rinsed with PBS solution for three times. The final products were stored in PBS solution at 4 °C for further use.

2.2.3 Functionalization with CD271 antibody (CD271/PDA/CS)

(+)-Biotin N-hydroxysuccinimide ester (biotin-NHS) (Abcam, Cambridge, USA) was added to PBS-DMSO (SIGMA-ALDRICH, St. Louis, USA) mixture solution (3:1) at a concentration of 1 mg/mL to prepare the biotin-NHS solution. Both chitosan microspheres and PDA coated chitosan microspheres were immersed in the biotin-NHS solution under stirring at room temperature for 3 hours and then collected and washed by PBS solution for three times. DyLight® 488 streptavidin (SAV) (Biolegend, San Diego, USA) was used to confirm the successful reaction with biotin-NHS. Reacted microspheres were immersed in DyLight® 488 SAV solution (5 μg/mL) for 15 minutes and were washed with PBS to remove unreacted SAV. Blank CS and PDA/CS microspheres were reacted with DyLight® 488 SAV in the same way as control. The microspheres were then observed using a fluorescence microscope (Zeiss Axiovert 200, Carl Zeiss Inc., New York, USA).

The prepared biotin/CS microspheres and biotin/PDA/CS microspheres were immersed in SAV (dissolved in PBS, 50 μg/mL) (SIGMA-ALDRICH, St. Louis, USA) solution for 15 minutes at room temperature respectively to introduce SAV to the surface of microspheres. PBS was used to wash off the unreacted SAV. Then the microspheres were further incubated with biotinylated CD271 antibody (4.17 μg/mL) (BD Biosciences, New Jersey, USA) under stirring for 15 minutes at room temperature. The final products were rinsed by PBS for three times. A secondary labeled antibody Cy3 (Invitrogen, Waltham, USA) was used to evaluate the results of antibody conjunction. SAV/CS microspheres and SAV/PDA/CS

microspheres were treated by the secondary labeled antibody Cy3 in the same way as control. The microspheres were then observed using a fluorescence microscope. After confirming the conjugation of CD271 antibody, we adjusted the amount of PBS solution to achieve the concentration of about 100 microspheres per 100 μL PBS under the condition of uniform suspension for storage at 4 ° C.

2.2.4 Scanning electron microscopy

The CS microspheres and PDA/CS microspheres were imaged using a scanning electron microscope (SEM, S-4800; Hitachi, Kotyo, Japan). After being immobilized on the SEM sample stubs, the samples were sputter coated with gold in a gold sputter coating equipment (SC7620, Quorum Technologies, UK) for 60 s. Then imaging was carried out under an accelerating voltage of 10 kV.

2.3. In vitro experiments

2.3.1 Cell culture

Human bone marrow mesenchymal stem cells (Cyagen, Guangzhou, China) were cultured in OriCell™ human mesenchymal stem cell growth medium (88% human mesenchymal stem cell basal medium, 10% human mesenchymal stem cell-qualified feta bovine serum, 1% penicillin-streptomycin, 1% glutamine) (Cyagen, Guangzhou, China). Similarly, SD rat bone marrow mesenchymal stem cells (Cyagen, Guangzhou, China) were cultured in OriCell™ mouse mesenchymal stem cell growth medium (88% mouse mesenchymal stem cell basal medium, 10% mouse mesenchymal stem cell-qualified feta bovine serum, 1% penicillin-streptomycin, 1% glutamine) (Cyagen, Guangzhou, China). Culturing media was changed every two or three days. Cells were trypsinized to passage when reaching 80% confluence, and the cells in passage 2-7 were used (only passage 2-3 were used in the formal experiment). Human peripheral blood mononuclear cells (hPBMCs) were kindly gifted from Dr. Qin Shi's lab and

were cultured in RPMI-1640 media (Hyclone, Logan, USA). Cells in passage 1 were used. All these cells were cultured in a 37 °C incubator with 5% CO_2.

2.3.2 Immunocytochemistry

hBM-MSCs were fixed by 4% paraformaldehyde (Biosharp, Shanghai, China) for 20 minutes and then blocked by 2% bovine serum albumin (BSA) (Biosharp, Shanghai, China) for 2 hours at 4 °C. After incubation with 2 μg/mL FITC-labeled CD271 antibody (Biolegend, San Diego, USA) in 4 °C overnight, the cells were further treated with 0.1 μg/mL DAPI (Roche, Basel, Switzerland) solution for 20 minutes at room temperature to stain the nuclei. Then the cells were observed using the fluorescent microscope. hBM-MSCs were also stained by PE-CD34 (eBioscience, San Diego, USA) antibody in the same way as control.

2.3.3 Flow cytometry

Cells (1×10^6 / sample) were fixed with 4% paraformaldehyde for 20 minutes and then treated by 2% BSA for 2 hours to block non-specific protein-protein interactions. Then the cells were incubated with 1/10 dilution FITC-labeled CD271 antibody (Biolegend, San Diego, USA) at room temperature for 30 minutes. FITC-labeled mouse IgG1 (Abcam, Cambridge, USA) antibody was used as isotype control. The labeled cells were detected by the fluorescence-activated cell sorter (FACSAria III, BD Biosciences , New Jersey, USA).

2.3.4 Cell capture experiment

hBM-MSCs were trypsinized and resuspended by medium at the concentration of 10^6 cells/mL. Then the cells were incubated with 1, 1'-Dioctadecyl-3, 3, 3', 3'-tetramethylindocarbocyanine perchlorate (Dig, 5 μL/mL, KeyGEN BioTECH, Nanjin, China) in incubator for 20 minutes. After

washing, the pre-stained hBM-MSCs were then incubated with different microspheres at a density of about 50 cells per particle in non-adherent 6-well plate for 6 hours in the 37 °C incubator with 5% CO_2. Specifically, the aformentioned microsphere storage solution was first blow sufficiently to make the microsphere suspension evenly, and then suck out 1000 μL solution into cell culture plate. Then, the microspheres were counted under the optical microscope and adjusted to 1000 microspheres per well. After the PBS solution was sucked out, 5×10^5 hBM-BMSCs were added into the cell culture plate to reach the density of 50 cells per particle. Four kinds of microspheres were studied, including CD271/PDA/CS, CD271/CS, PDA/CS, and CS microspheres. After incubation, a 40 μm strainer (Corning, New York, USA) was used to filter out the uncaptured cells. The capturing result was evaluated using fluorescent microscope. The CellTiter 96® AQueous One Solution Cell Proliferation Assay (MTS, Promega, Madison, USA) was also used to quantitatively analyze the results of cell capture experiment according to the manufacturer's instructions..

2.3.5 Cell expansion experiment

The captured cells were further cultured in 6-well plate for 21 days to study the cell expansion on different microspheres. At day 1, 10 and 21, microspheres with cells were fixed with 4% paraformaldehyde for 20 minutes and then blocked by 2% BSA for 2 hours at room temperature. The samples were stained by 5 μg/mL FITC-phalloidin (Cytoskeleton, Denver, USA) and DAPI sequentially for 20 minutes, and were then observed by the fluorescent microscope. MTS assay was performed at day 1, 7, 14, 21 to quantitatively analyze the expansion of cells in different groups.

2.3.6 MTS assay

One hundred microspheres of each group were placed in 100 μL human mesenchymal stem cell

growth medium on 96-well plates. Blank well with culture medium only was used as blank control. Then, 20 μL MTS reagent (Promega, Madison, USA) was added to each well and the plate was cultured in the 37 °C incubator with 5% CO_2 for 3 hours. Afterwards 100 μL cultured medium was taken from each well and moved to a new 96-well plate. The absorbance at 490 nm was read by a microplate reader (Bio Tek, Winooski, Vermont, USA). The results were obtained by subtracting the absorbance of each sample well with the mean value of blank wells.

2.3.7 Cell isolation experiment

For easy observation, hBM-MSCs and hPBMCs were pre-stained with 3, 3'-Dioctadecyloxacarbocyanine perchlorate (DiO) (KeyGEN BioTECH, Nanjin, China) and DiI respectively. Then the stained hBM-MSCs and hPBMCs were mixed at a ratio of 1:1 to form heterotypic cell suspension. CD271/PDA/CS microspheres, CD271/CS microspheres, PDA/CS microspheres, and CS microspheres were incubated with same amount of heterotypic cell suspension in non-adherent 6-well plate at 37 °C with 5% CO_2. After 3 hours of incubation, the suspension of cells and microspheres were filtered with a 40 μm strainer and then observed using the fluorescence microscope. The microspheres in each group were further trypsinized to collect cells. The collected cells were mote into 48-well plates. The number of hBM-MSCs and hPBMCs in each unite area were counted under the fluorescence microscope. Nine areas were counted per well. The total amount of captured hBM-MSCs and hPBMCs in each group were estimated by the mean number of cells in nine areas, the area of observation unit, and the total area of each well.

2.4. In vivo experiments

2.4.1 In situ recruitment of $CD271^+$ stem cells

All procedures were approved by the Institutional Animal Care and Use Committee of Soochow University with applying Chinese national guidelines for the care and use of laboratory animals. Male Sprague-Dawley (SD) rats with weight of 250 g (purchased from the Experimental Animal Center of Soochow University, Suzhou, China) were anesthetized with isoflurane inhalation (600 mL/min). A defect with the width of 2.5 mm and depth of 3 mm was then created on the femoral lateral condyle. The defects were then full filled with CD271/PDA/CS microspheres, CD271/CS microspheres, PDA/CS microspheres, or CS microspheres. The rats were sacrificed at day 3 and day 7. The femoral bone tissues were collected and fixed in 4% paraformaldehyde solution and microspheres were taken out from the defect. After being blocked by 2% bovine serum albumin (BSA) for 1 h at room temperature, samples were incubated with 2 μg/mL FITC-labeled CD271 antibody in 4 °C overnight along with being further treated anti-fluorescence quenching sealing solution (including DAPI) (Beyotime, Shanghai, China) for 5 minutes at room temperature to stain the nuclei. Then the cells were observed using the laser scanning confocal microscopy (FV3000, Olympus, Tokyo, Japan).

2.4.2 Bone defect regeneration

Male Sprague-Dawley (SD) rats with weight of 250 g (purchased from the Experimental Animal Center of Soochow University, Suzhou, China) were used. Before surgery, anesthesia was carried out by intraperitoneal injection of 2% pentobarbital sodium (Shanghai Pharma New Asia Phamaceutical Co., Ltd, Shanghai, China,). A defect with the diameter of 2.5 mm and depth of 3 mm was then created in the femoral condyle. After the sucking up the PBS used to soak the microspheres, a sterile spoon was applied to move the microspheres into the femoral condyle defect, and at the same time fully compacted until the entire defect cavity was completely filled with microspheres (58.93 mm^3 microspheres per defect area).

Then the defect site was covered with muscles and closed with soft tissues layer by layer. Then the same surgery was repeated in the other leg of the rat. The kind of microsphere (CD271/PDA/CS microspheres, CD271/CS microspheres, PDA/CS microspheres, CS microspheres, blank control, or sham) filled to each defect was decided by a randomized manner. Each kind of microspheres were filled to a total of 8 rats, with 4 rats per time point (6 weeks and 12 weeks) (Table S1). Penicillin was intramuscularly injected to all rats to prevent infection. No rat was loss during the study. All surgical procedures were approved by the Institutional Animal Care and Use Committee of Soochow University with applying Chinese national guidelines for the care and use of laboratory animals.

2.4.3 Micro-computed tomography evaluation

At 6 and 12 weeks after implantation, the animals were sacrificed by overdose anesthesia. The femurs were harvested. The samples were scanned with Micro-computed tomography (micro-CT) (SkyScan 1176, SkyScan, Aartselaar, Belgium), and the matching software was used to carry out three dimensional (3D) reconstruction of tissue and the calculation of bone volume fraction (bone volume/ tissue volume, i.e, BV/TV). Trabecular bone related analyses, such as trabecular thickness (Tb. Th), trabecular number, and trabecular pattern factor (Tb. Pf), were also performed.

2.4.4 Histological assessment

The harvested samples were fixed with 4% paraformaldehyde for 2 days, and decalcified by 0.5M ethylenediaminetetraacetic acid (EDTA) at room temperature for 2 weeks. After being embedded in paraffin blocks, the samples were sectioned with thickness of 5 μm and stained with hematoxylin and eosin (H&E) for light microscopic analysis. Bright field microscope (Zeiss Axiovert 200, Carl Zeiss Inc., New York, USA) was used to capture the images.

2.5 Statistical analysis

All *in vitro* experiments were performed in at least triplicate. Data were expressed in the form of means ± SD. Statistical comparisons were performed by one-way ANOVA, two-way ANOVA, or Student's t-tests with SPSS 16.0 software (SPSS, USA). For data that did not conform to the normal distribution, the corresponding figure was replotted with dot plots, and the nonparametric detection was used. A difference with $p < 0.05$ was considered statistically significant.

3. Results and Disscussion

3.1 Fabrication of CD271 antibody conjugated microspheres

Droplets of chitosan solution was generated by the high-voltage electrostatic field and then harden by the sodium hydroxide solution (Fig. S1). A filter was used to sift out the microspheres that were too small for cell to attach and expand. The diameter of the filtered microspheres ranged from about 100 μm to 500 μm (Fig. 1A and 1B). The histogram of the distribution of microparticles were showed in Fig. S2, which revealed that a total of 77.68% microspheres ranged from 340 to 440 μm. The diameter of submicron provided high surface area for cell attachment. Polydopamine (PDA) coating was then deposited onto CS microspheres by polymerizing dopamine in 10 mM Tris-HCl buffer (pH = 8.5) (PDA/CS), and the color of the transparent microspheres turned black (Fig. 1C and 1D) [40, 42]. The SEM images showed that the surface of PDA/CS microsphere (Fig. 1G and 1H) was much rougher than that of CS microsphere (Fig. 1E and 1F).

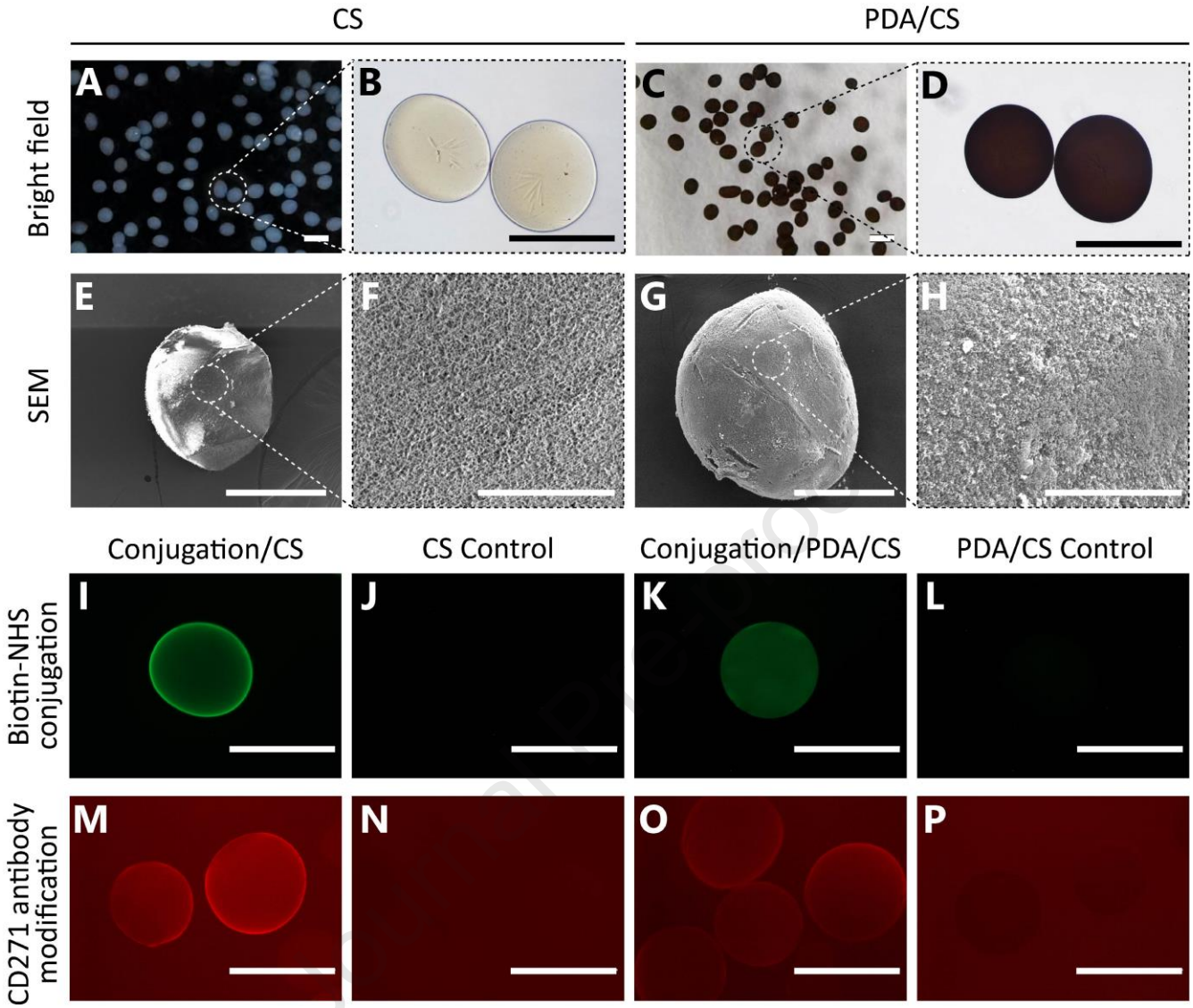

Fig. 1. Preparation of the functional microspheres. The gross appearance (A), optical microscopy image (B) of chitosan microspheres and the gross appearance (C), optical microscopy image (D) of PDA coated chitosan microspheres. SEM images of chitosan microspheres (E) and (F) and PDA coated chitosan microspheres (G) and (H). Fluorescence images of NHS-biotin modified CS microsphere (I) and PDA/CS microsphere (K) after incubation with DyLight® 488 SAV, and fluorescence images of pristine CS microsphere (J) and PDA/CS microsphere (L) after incubation with DyLight® 488 SAV as control. Fluorescence images of CD271/CS microsphere (M) and CD271/PDA/CS microsphere (O) after

incubation with a secondary labeled antibody Cy3, and fluorescence images of SAV/CS microsphere (N) and SAV/PDA/CS microsphere (P) after incubation with a secondary labeled antibody Cy3 as control. Scale bars, 400 μm (A-D, and I-P), 200 μm (E and G), and 30μm (F and H).

The PDA/CS microspheres were then functionalized with CD271 antibody using biotin-SAV interactions. Biotin-SAV interaction is considered as one of the strongest non-covalent interactions in nature with an extremely low dissociation constant K_d of about 10^{-14} M[47], and this grafting strategy is also expected to improve the freedom and activity of the grafted CD271 antibody. Free amine reactive groups on the surface of the particles were used to tether biotin through the biotin-NHS. DyLight 488 SAV was used to indirectly evaluate the efficiency of the connection between biotin-NHS and microspheres. Green fluorescence could be observed in both biotin/CS microspheres (Fig. 1I) and biotin/PDA/CS microspheres (Fig. 1K), but absence in unmodified CS microspheres (Fig. 1J) and PDA/CS microspheres (Fig. 1L), indicating the specific binding of biotin-NHS and microspheres.

As mentioned above, biotin-CD271 antibody was then connected to biotin modified microspheres through the SAV. The modification of CD271 antibody was assessed by a secondary labeled antibody Cy3. As showed in Fig. 1M and 1O, CD271/CS microspheres and CD271/PDA/CS microspheres both revealed red fluorescence under fluorescent microscope, whereas no fluorescence was found in SAV/CS group and SAV/PDA/CS group (Fig. 1N and 1P). It is worth noting that the microspheres in Fig. 1J and 1N did not reveal the non-specific fluorescence as in the fluorescence pictures of the subsequent experiments. This is because the fluorescence of the experimental group is so strong that only a very small amount of laser excitation was needed. These results demonstrated that microspheres were

successfully and specifically modified with CD271 antibody.

3.2 CD271 expression in different kinds of cells

CD271 expression in different kinds of cells were detected. Green fluorescence could be observed in part of hBM-MSCs (Fig. 2A) after stained by FITC-labeled CD271 antibody (IgG1 isotype control antibody (Fig. 2B) and PE-labeled CD34 antibody (Fig. S3) were used as negative control), indicating a partly positive expression of CD271 antigen in hBM-MSCs of P2 generation. The outcome of flow cytometry further confirmed this result and revealed that the expression ratio was 25.4% (Fig. 2C), which was consistent with the literature [48]. It has also been confirmed that part of rat BM-MSCs of P3 generation express CD271 antigen (Fig. S4), which laid the foundation for our subsequent *in vivo* experiments. These results demonstrated that a number of CD271 antigens existed on the surface of both hBM-MSCs and rat BM-MSCs that could be specifically recognized by the CD271 antibody. In fact, studies have found that the percentage of $CD90^+CD105^+CD45^+CD34^+CD79^+$ cells in bone marrow mononuclear cells coincided with the amount of $CD271^+$ cell subset (0.54%) *in vivo* [49]. However, the expressions of CD271 antigen in BM-MSCs from two species were relatively low in our study. This result is mainly due to that after the *in vitro* culture and passage, the expression of CD271 antigen in BM-MSCs will gradually decrease [48, 50]. However, due to the existence of a certain number of $CD271^+$ cells, the cultured BM-BMSCs are still suitable for related *in vitro* experiments. Moreover, Fig. 2E showed that CD271 was lowly expressed in hPBMCs (2.8%) [51], which made it suitable to constitute a heterotypic cell suspension with BM-MSCs to detect the specificity of CD271 antibody *in vitro* (Fig. 2E).

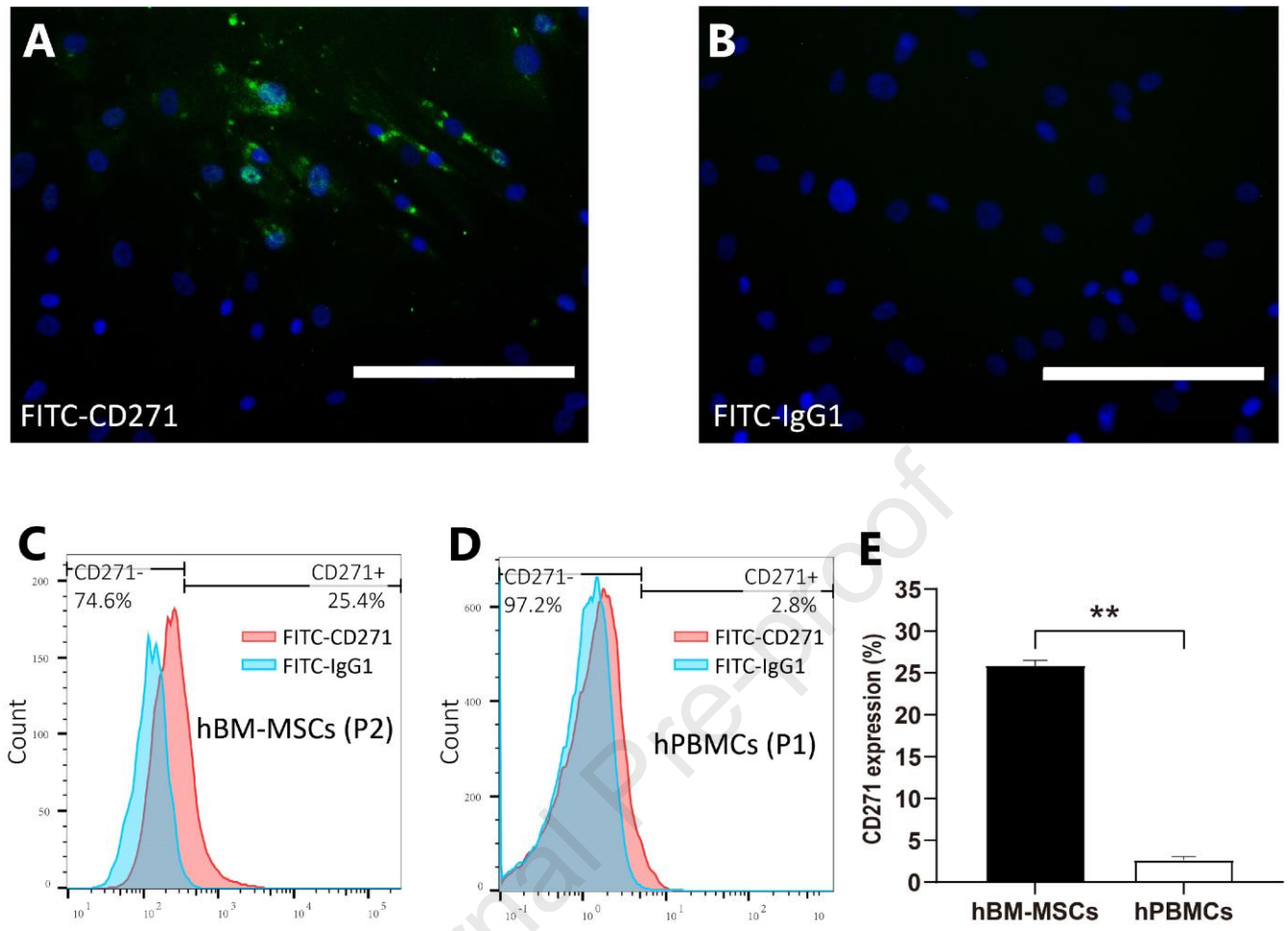

Fig. 2. The expression of CD271 in different kinds of cells. Immunofluorescence assays of hBM-MSCs (P2) stained by FITC-CD271 (A) and FITC-IgG1 Isotype control (B); flow cytometry analysis of hBM-MSCs (C) and hPBMCs (D) after incubation with FITC-CD271 antibody and FITC-IgG1 isotype control antibody, and the comparison of CD271 expression between the two groups (E). Scale bars, 400 μm. ** $p < 0.01$.

3.3 In vitro cell capture experiment

The capture of hBM-MSCs was induced by the highly specific interactions between the CD271 antigen in hBM-MSCs and the CD271 antibody on the microspheres. Cells were pre-stained fluorescent

tags for easier observation. After 5 hours of co-incubation, a large number of captured hBM-MSCs could be found in CD271/PDA/CS group (Fig. 3A) and CD271/CS group (Fig. 3B), while little was found in CS control group (Fig. 3D). The number of cells attaching on PDA/CS microspheres was more than that on CS microspheres but less than that on CD271/PDA/CS microspheres and CD271/CS microspheres (Fig. 3C). It seems that the numbers of BM-BMSCs captured by CD271/PDA/CS, CD271/CS and PDA/CS groups were all higher than the theoretical number, which might be attributed to the non-specific adsorption of microspheres, especially that the PDA coating in CD271/PDA/CS group and PDA/CS group could provide high adhesion. Result of MTS assay was shown in Fig. 3E. It can be found that CD271/PDA/CS group and CD271/CS group could capture much more cells than PDA/CS group and CS group. Despite the number of captured cells in CD271/PDA/CS group was more than that in CD271/CS group, no statistic difference was revealed ($p > 0.05$). The similar result can be found between PDA/CS group and CS group ($p > 0.05$). These experiments preliminarily proved that CD271 antibody can help the microspheres capture BM-MSCs from a homogenous cell environment.

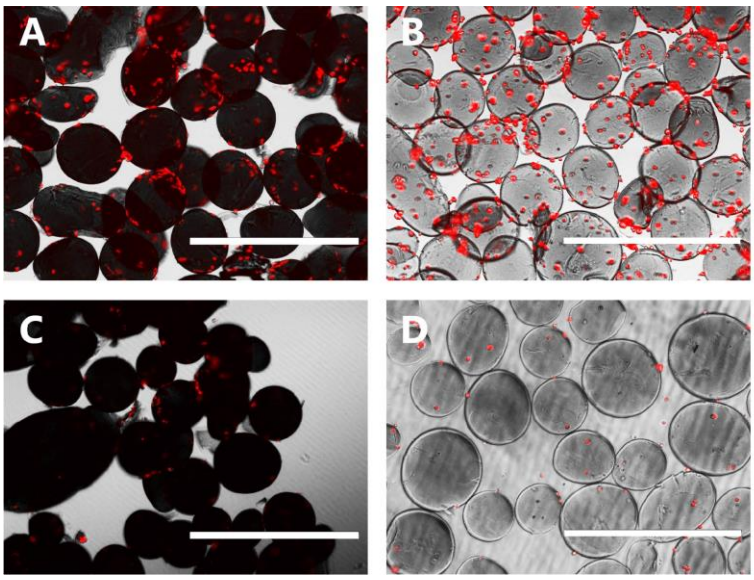

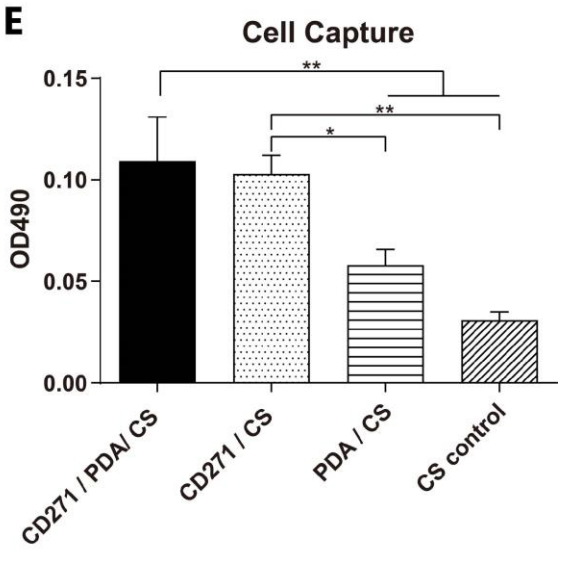

Fig. 3. Capability of microspheres in capturing hBM-MSCs. Immunofluorescence image of captured hBM-MSCs (stained red) on CD271/PDA/CS microspheres (A), CD271/CS microspheres (B), PDA/CS microspheres (C), and CS microspheres (D); (E) MTS assays characterizing the hBM-MSC capture capability of different microspheres. Scale bars, 1000 μm. *$p < 0.05$ and **$p < 0.01$.

3.4 Cell expansion experiment

The morphology of cells on the surface of microspheres was evaluated through DAPI and FITC-phalloidine staining in day 1, 10, and 21. Results (Fig. 4A) showed that the morphology of hBM-MSCs on CD271/CS microspheres and CS microspheres was globose rather than fusiform. Moreover, the number of cells in CD271/CS group gradually decreased. In day 10 only a few cells could be observed on the surface of CD271/CS microspheres and in day 21 the cells could hardly be found. Similar trend could also be observed in CS group. We attributed the poor results of CD271/CS group and CS group to the smooth cambered surface and microenvironment of CS microsphere. The PDA coating seemed to sucesuffly solve the problem, as fusiform cells attaching on the surface of microspheres with obvious proliferation could be observed in CD271/PDA/CS group. In day 21 the cells were almost 80% confluent. Results revealed that gradual expansion of hBM-MSCs could also be found in PDA/CS group despite the initial number of cells was much lower.

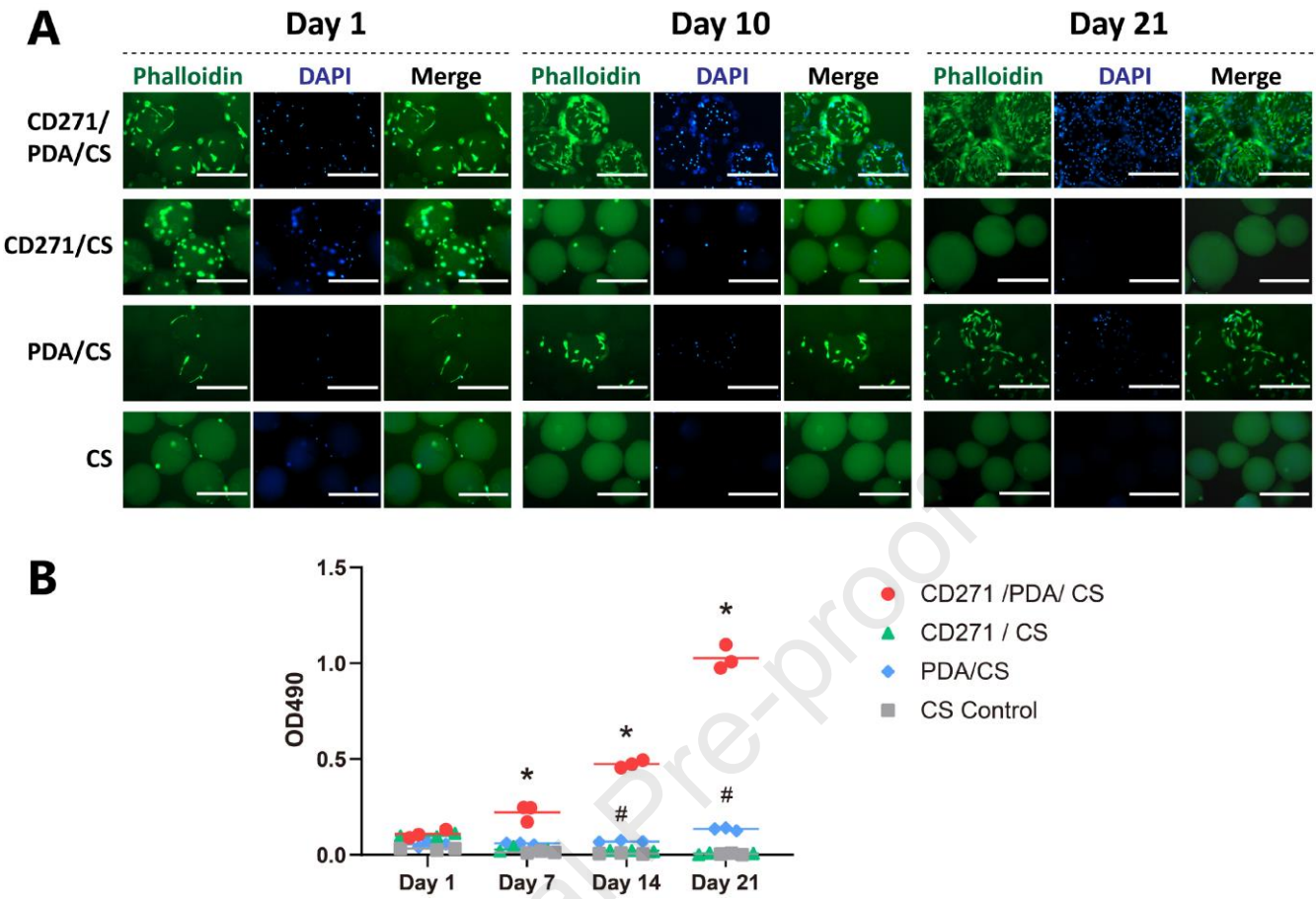

Fig. 4. Cell attachment and proliferation on microspheres. (A) Immunofluorescent images of hBM-MSCs on CD271/PDA/CS microspheres, CD271/CS microspheres, PDA/CS microspheres, and CS microspheres after seeding for 1 day, 10 days, and 21 days. Scale bars, 400 μm. (B) MTS assay of the proliferation of hBM-MSCs on different microspheres (n = 3). * $p < 0.05$ for CD271/PDA/CS versus CD271/CS and CS, # $p < 0.05$ for PDA/CS versus CD271/CS and CS.

The MTS assay revealed the similar result, which was shown in Fig. 4B. The OD value of CD271/CS group decreased to the level that was comparable to CS group in day 7, indicating mass of hBM-MSCs dropping from the surface of the microspheres. Whereas in CD271/PDA/CS group and PDA/CS group the OD value gradually increased over time. The OD value of CD271/PDA/CS group in

day 21 was almost 10 time of that in day 1. The expansion speed in PDA/CS group was much slower than CD271/PDA/CS group, and at each time point the OD value of PDA/CS group was far lower. It seems that the PDA coating could provide a suitable surface for cells well attaching and expanding.

The possible reason for the promising results of cell attachment and proliferation on PDA groups is that the PDA coating contains highly hydrophilicity and bioactive groups as OH^- and NH_2^- [52, 53] , and can immobilize serum adhesive proteins [54]. Studies also found that the PDA coating could serve as a platform for secondary modification, such as introduce metal and bioceramic by spontaneous deposition [42, 55]. So we could connect other functional groups to our microsphere through the PDA coating for diverse functional uses in the future.

3.5 In vitro cell isolation experiment

It is well known that there are many other types of cells besides BM-MSCs in bone marrow. So heterogeneous cell population was used to evaluate the ability of our functional microspheres to specifically capture target cells. We chose hPBMCs and hBM-MSCs to form the heterogeneous cell population. The hPBMCs contained lymphocytes, monocytes, dendritic cells, and a small amount of hematopoietic stem cells, which could, to some extent, mimic the cellular environment of bone marrow. More importantly, the expression of CD271 antigen in PBMCs was very low [51]. For easier observation, hBM-MSCs were pre-stained with green fluorescence and hPBMCs were pre-stained with red fluorescence. The revelent results were exhibited in Fig. 5A. Through the fluorescent microscope it can be found that there was little hBM-MSCs and hPBMSCs in CS microspheres, and there were lots of hBM-MSCs but little hPBMSCs in CD271/PDA/CS microspheres and CD271/CS microspheres. As to

PDA/CS group, the captured hBM-MSCs was more than CS group but less than CD271/PDA/CS group and CD271/CS group. Compared with CS group and CD271/CS group more hPBMCs could be found in CD271/PDA/CS group and PDA/CS group. No significant visual difference about the number of hPBMSCs was found in the two PDA coated groups or the two groups without PDA coating.

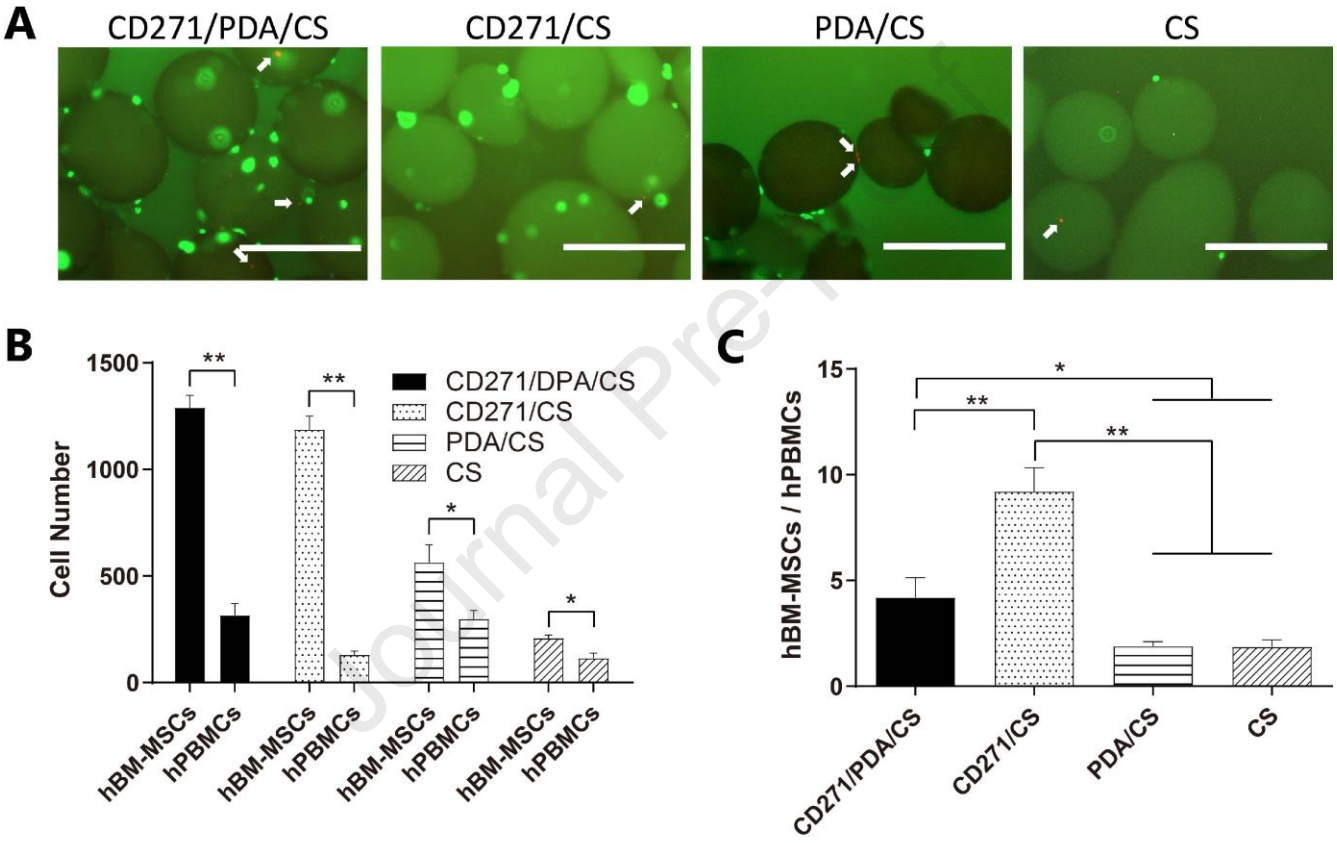

Fig. 5. Cell isolation assays. (A) Immunofluorescence images of captured hBM-MSCs (stained green) and hPBMCs (stained red) on different microspheres from heterotypic cell population of 1:1 hBM-MSCs and hPBMCs (white arrow shows hPBMCs). (B) Histogram of the number of captured hBM-MSCs and hPBMCs on different microspheres (n = 3); (C) the ratio of hBM-MSCs/hPBMCs in each group (n = 3).

Scale bars, 400 μm, respectively. The white arrows point to red dots (hPBMCs). * $p < 0.05$ and ** $p < 0.01$.

The result of quantitative analysis showed in Fig. 5B. It can be found that the number of hBM-MSCs in CD271/PDA/CS group (1289.71 ± 57.79 hBM-MSCs) and CD271/CS group (1186.38 ± 63.23 hBM-MSCs) was far more than that in PDA/CSgroup (562.57 ± 82.79 hBM-MSCs) and CS group (208.57 ± 14.44 hBM-MSCs), while PDA/CS group held more hBM-MSCs than CS group. This trend was similar to the cell capture experiment. Additionally, PDA/CS microspheres captured approximately two times of hPBMCs (298.51 ± 39.77 hPBMCs) compared with CS microspheres (114.81 ± 22.96 hPBMSCs). This might because the nonspecific adsorption of the PDA coating. So the CD271 antibody could help to specifically recruit hBM-MSCs from a heterogeneous cell population. The ratio of captured hBM-MSCs and hPBMCs in each group was calculated to evaluate the specificity of isolation. As shown in Fig. 5C, the CD271/CS group (hBM-MSCs:hPBMSCs = 9.21:1) held the highest ratio while the CD271/PDA/CS group (hBM-MSCs:hPBMSCs = 4.19:1) held the second. So the PDA coating partly influenced the specificity of recruitment. Whereas the result of CD271/PDA/CS group was much better than PDA/CS group (hBM-MSCs:hPBMSCs = 1.89:1) ($p < 0.05$) and CS group (hBM-MSCs:hPBMSCs = 1.85:1) ($p < 0.05$), indicating that our functional system was still satisfactory in capturing the target hBM-MSCs from the heterogeneous cell population.

3.6 In vivo cell recruitment

In vivo performance of the targeted cell recruitment was also evaluated using the rat model of lateral

femoral condyle defect [56]. On the third and seventh day after implantation, the microspheres were removed, followed by immunofluorescence staining with FITC labeled CD271 antibody and DAPI to observe the recruitment of $CD271^+$ stem cells on and around the microspheres. Shown in Figure 6B are the fluorescence images of microspheres at 3 and 7 days after implantation. Green fluorescence indicating $CD271^+$ stem cells could be clearly observed on CD271/PDA/CS microspheres at Day 3 and the intensity significantly enhanced at Day 7, indicating a considerable number of recruited BM-MSCs on the CD271/PDA/CS microspheres. In comparison, much less green fluorescence was observed in the PDA/CS group, although many blue dots which indicating $CD271^-$ cells were found to attach on the microspheres. On the other hand, CD271/CS microspheres and CS microspheres had much less cells on their surface, while blue dot fluorescence mainly concentrated in the surrounding tissues. This result is consistent with the *in vitro* study, which may be due to the surface of chitosan microspheres without PDA coating is not suitable for cell adhesion and proliferation. It is worth noting that although green fluorescence can be observed on the surface of implanted CD271/CS microspheres and CS microspheres, it does not represent $CD271^+$ cells. This is because the green fluorescence on the surface of the microspheres is very uniform, which is consist with the microspheres before implantation (Fig. 6A). This phenomenon might be caused by the refraction of fluorescence from the transparent sphere. In the tissue around the microspheres, the number of green fluorescence in CD271/CS group was significantly more than that in CS group, and more $CD271^+$ cells could be observed in the 7^{th} day. Although we can hardly give the finally conclusion that all the cells showing green fluorescence are BM-MSCs, these results confirmed the effect of CD271 antibody on cell recruitment *in vivo*. On the other hand, these recruited cells were bound to contain large number of $CD271^+$ BM-MSCs colonies [49], and studies have found

that CD271$^+$ BM-MSCs held excellent osteogenic differentiation potential [26], which will also be verified from a side in the subsequent bone regeneration experiments.

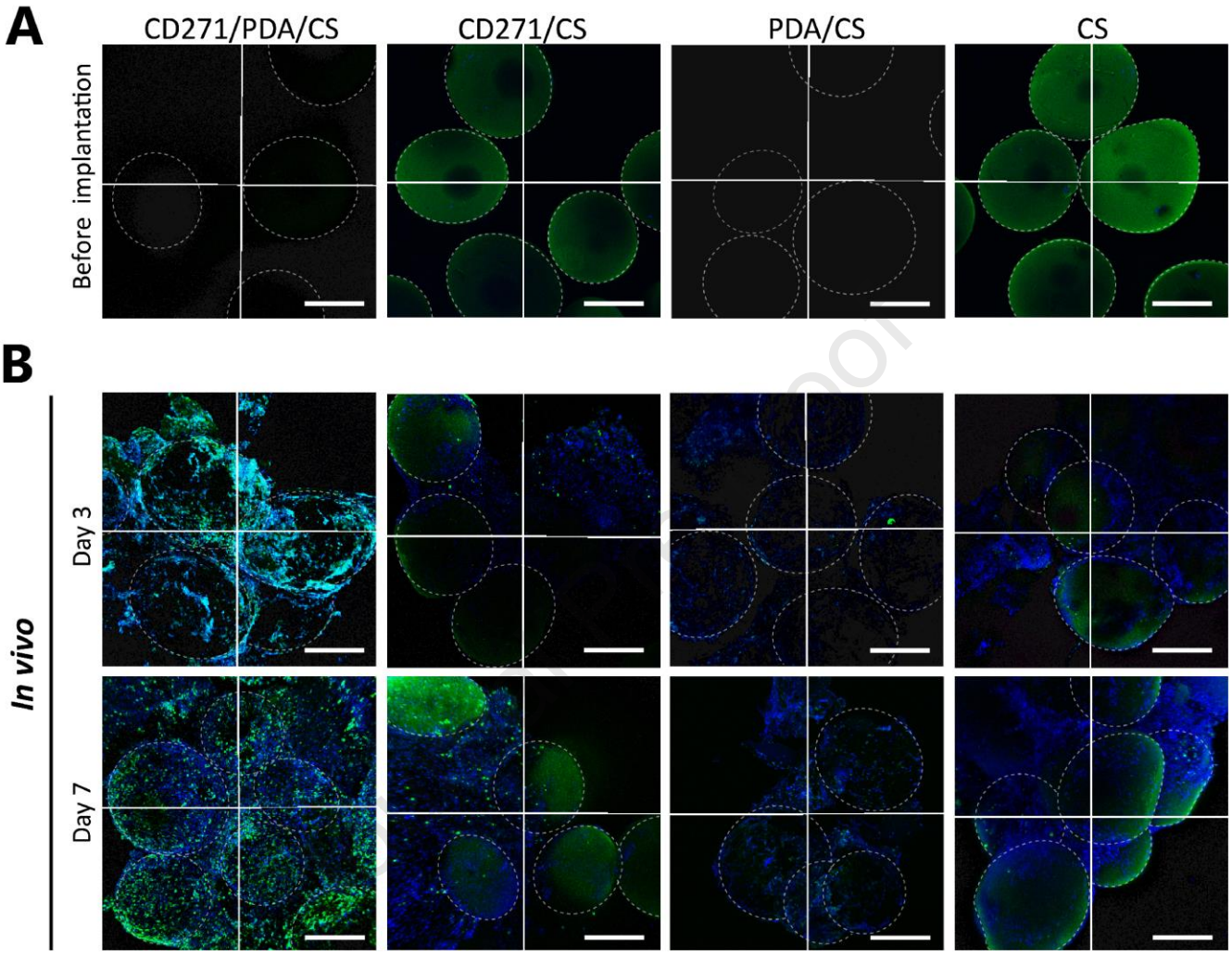

Fig. 6. *In vivo* cell recruitment. CD271/DAPI immunofluorescence images of various kinds of microspheres before implantation (A) or 3 days and 7 days after implantation *in vivo* (B). The green dots indicate the CD271$^+$ cells, the blue dots indicate nucleus of cells, and the white circles shows outlines of microspheres. Scale bars, 200 μm.

3.7 In vivo bone regeneration

Defects of femoral condyle in rats were surgically created to evaluate the ability of our functional

microspheres in facilitating bone formation *in vivo* (Fig. S5). Through the coronal and 3D reconstruction of micro-CT, obvious new bone formation at defect site could be found in CD271/PDA/CS group at 12 weeks. In other groups there were still apparent defects or relatively thin bone lamella (Fig. 7A). Bone volume per tissue volume (BV/TV) was used to quantitative measure the new bone tissue in each group, which was exhibited in Fig. 7B. The newly formed bone volume was highest in CD271/PDA/CS group in both 6 weeks (59.68 ± 3.65%) and 12 weeks (70.26 ± 2.48%), and the bone volume in 12 weeks was higher than that in 6 weeks, indicating the bone content in this group increased over time. Results of CD271/CS group (41.99 ± 4.36% at 6 weeks, and 49.69 ± 2.98% at 12 weeks) and PDA/CS group (42.14 ± 4.67% at 6 weeks, and 53.98 ± 6.86% at 12 weeks) were comparable and were both better than that of CS group (37.20 ± 4.99% at 6 weeks, and 40.45 ± 3.47% at 12 weeks) and blank control group (35.00 ± 4.98% at 6 weeks, and 39.07 ± 7.51% at 12 weeks). It should be noticed that the BV/TV in CD271/PDA/CS gourp was even higher than that in sham group (57.89 ± 7.30% at 6 weeks, and 60.80 ± 9.53% at 12 weeks), but unfortunatelly no statical difference was revealed. Analysis of trabecular bone related results at 12 weeks postoperatively also showed that the CD271/PDA/CS group held the highest trabecular thickness (Tb. Th, 0.4819 ± 0.09 mm) and trabecular number (Tb. N, 1.95 ± 0.16/mm), as well as the lowest trabecular pattern factor (Tb. Pf, -11.20 ± 1.93/mm) (Fig. S6).

Histological analyses showed abundant typical newly formed trabeculae bone in CD271/PDA/CS group at 12 weeks, which was obviously thicker than other groups. The trabeculae bone in PDA/CS group was much fewer than CD271/PDA/CS group. Interestingly, in the two PDA-coated groups, newly formed trabeculae bone fully filled the gaps among microspheres, and even penetrated through microspheres. As to CD271/CS group and CS group, fewer newly formed trabeculae bone could be found

around each microsphere. Instead, there was obvious osseous boundary around the microsphere bunch. We speculate that this was because the cells could hardly adhere and proliferate on the surface of CD271/CS and CS microspheres, so the microspheres were agglomerated and separated from the newly formed bone. Although a large number of microspheres were also observed in the unhealed bone defect area of PDA/CS group, it was different from the condition of CD271/CS group and CS group. The main reason for this phenomenon in PDA/CS group was due to the insufficient new bone formation that failure to fill the whole defect site. It can be found that the junction between the microsphere mass and the bone margin is not separated, instead a lot of trabecular bone grows through the microsphere. Moreover, lots of trabecular bone and microspheres also coexisted in the healed area concurrently, just as in the CD271/PDA/CS group. These results imply that the PDA coating for supporting adhesion and expansion of BM-MSCs on microspheres is critically important. The thickness of the boundary in CD271/CS group was higher than CS group (Fig. 7C), which was consistent with the trend between the CD271/PDA/CS group and PDA/CS group. The Masson staining showed similar result (Fig. 7D). All these results demonstrate the critical role of the synergistic combination of CD271 antibody and PDA coating in promoting *in situ* bone regeneration (Scheme 1).

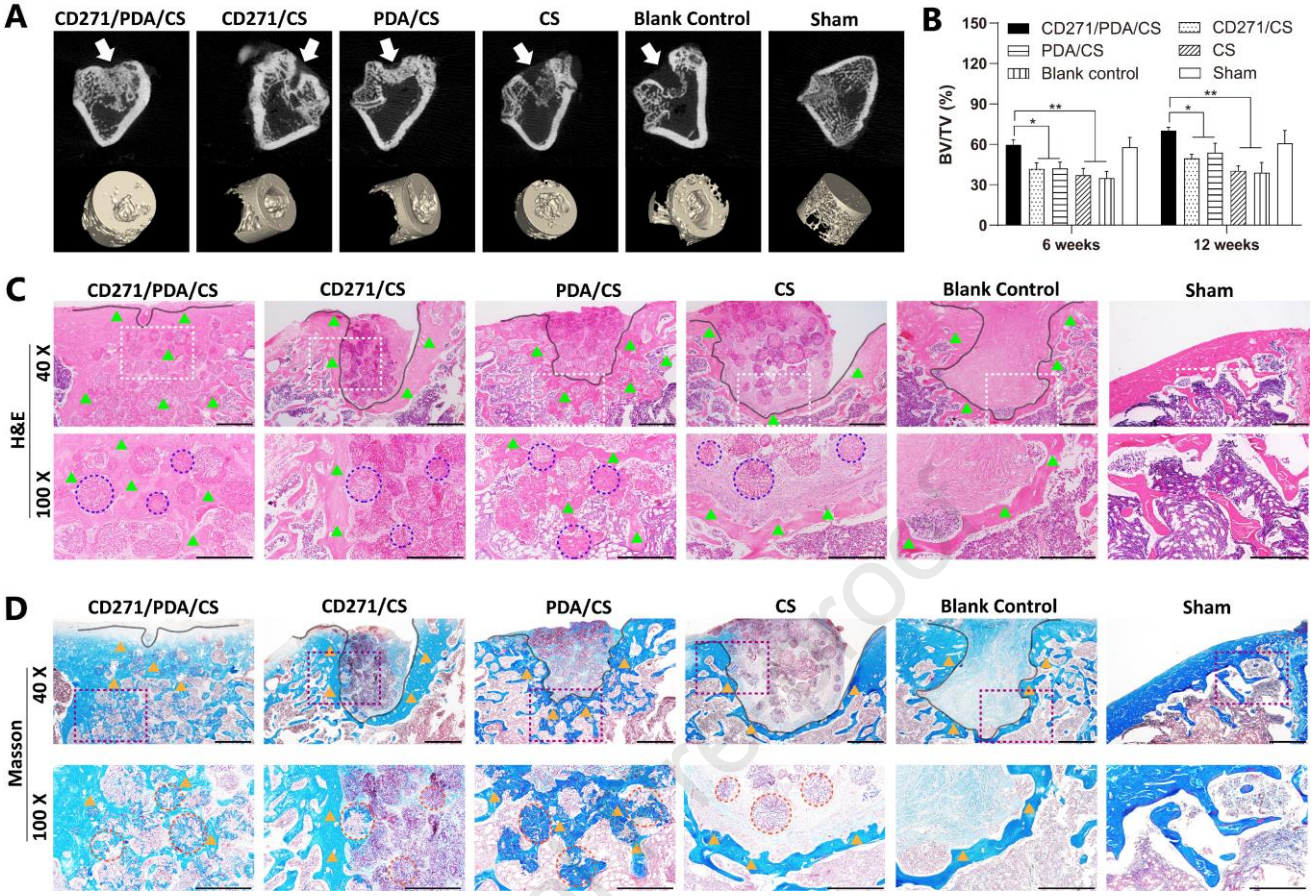

Fig. 7. Results of in vivo bone repair tests. (A) Coronal 3D reconstruction micro-CT images at 12 weeks. The white arrows indicate the defect sites. (B) Calculated bone volume faction (n = 4) in each group. Histomorphological analysis of rat femoral condyle at 12 weeks after operation with H&E staining (C) and Masson staining (D). The second row represents higher-magnification images (100×) of the corresponding white (C) or purple (D) square boxes in the upper row. The black curves outline the boundary of the residual bone defect after repair (C and D), the green (C) or yellow (D) triangles indicate newly formed trabecular bone tissues, and the blue (C) or red (D) circles shows remnant of microspheres. Scale bars, 1000 μm for 40× and 500 μm for 100×. * $p < 0.05$ and ** $p < 0.01$.

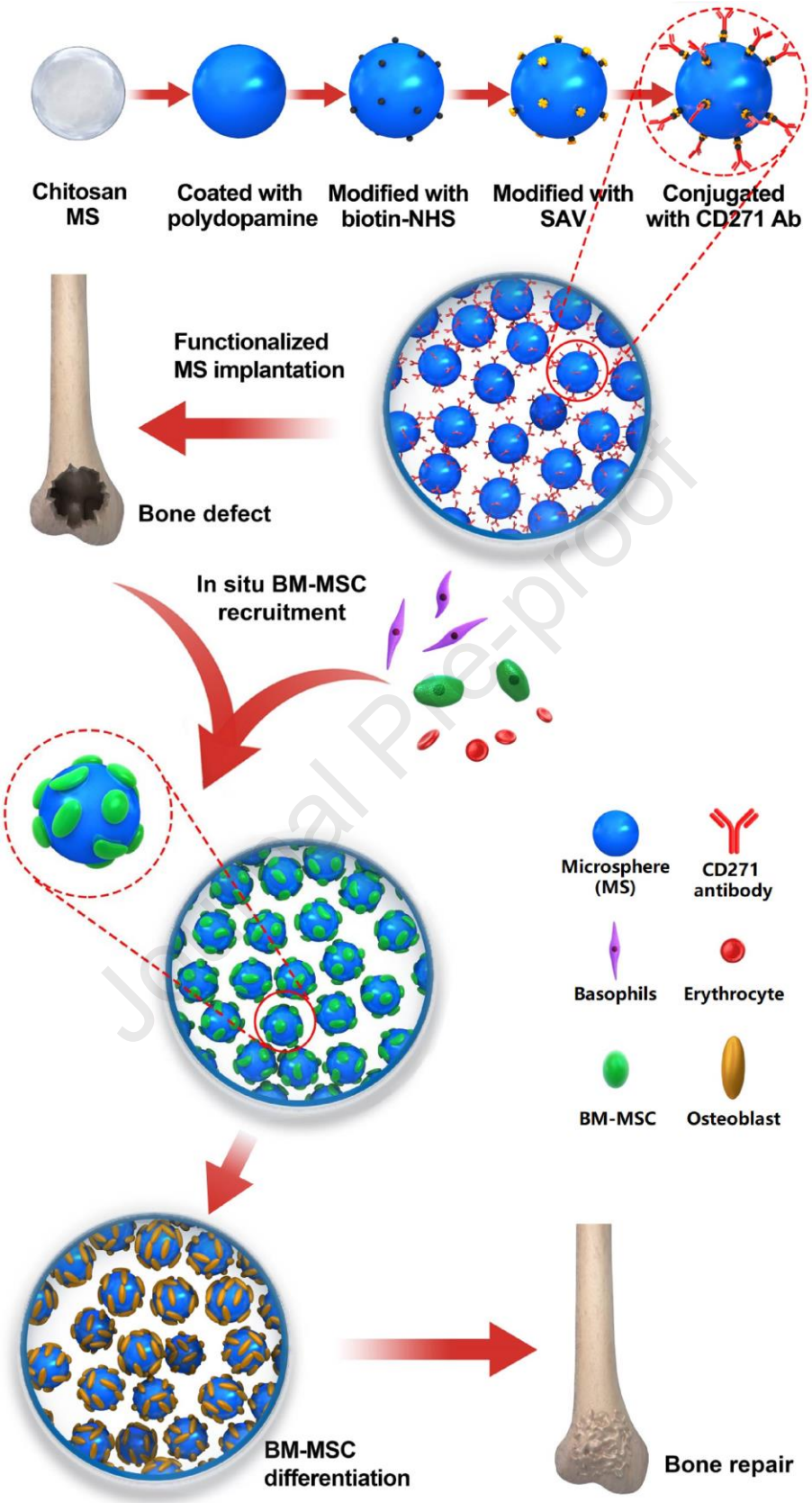

Scheme 1. Schematic illustration *of in vivo* recruitment of BM-MSCs on CD271-functionalized chitosan microspheres for *in situ* bone regeneration.

3.8 Limitations

There are still some limitations in this study. First of all, we only explored the feasibility of using CD271 antibody for specific recruitment, but did not explore the relationship between antibody dose and recruitment efficiency. Additionally, the cell types in mixed cell suspension used in the *in vitro* recruitment experiment were limited, and the cell proportion needs to be further optimized. The selective capturing of BM-MSCs against PBMCs was <5 in the CD271/DPA/CS group, which might be further improved by the surface modification of the microspheres to reduce the non-specific adhesion of cells. Moreover, we did not detect the stemness of the cells recruited *in vivo*. Finally, after 12 weeks, the bone defect was failed to be fully repaired by CD271/PDA/CS. We speculate that this is partly because our system lacks the function of inducing the recruited cells to differentiate into osteoblasts. On the other hand, most of the microspheres failed to be completely degraded. Therefore, in the future, osteogenic inducing growth factor can be added into our microspheres, which are made by novel material with suitable degradation time, to further enhance the ability of promoting bone regeneration and repair.

Conclusions

In summary, we have demonstrated the first example of CD271-functionalized chitosan microspheres for highly efficient *in situ* bone regeneration. It was demonstrated that with the help of CD271 antibody our functional microspheres could capture hBM-MSCs from the surrounding environment, and by the assistance of PDA coating the captured cells could well stretch and proliferate on the surface of microspheres. The CD271 antibody could also serve as the isolating factor to specifically recruit hBM-MSCs from a heterogeneous cell suspension. Finally, we confirmed the effect

of CD271 antibody on cell recruitment *in vivo*, and verified that our functional microspheres was satisfactory in facilitating bone regeneration. Therefore, our multifunctional CD271/PDA/CS microspheres are promising carriers for achieving *in situ* bone regeneration and more investigation should be conducted toward clinical applications. Our results also provide valuable insights into the mechanism of targeted recruitment of specific cells, which holds great potential to regenerating other types of tissue and organs.

Conflicts of interest

The authors declare no conflicts of interest.

Author contributions

BL, WS and HS conceived the idea. HS, QG, CS designed and performed the experiments. JC, CZ, FH, BM and HY supervised the study. HS, QG and PZ performed the experiments and analyzed the data. RHM, JL, XS helped analyze the data and provided valuable advices. HS and CS wrote the manuscript. BL, WS and RHM revised the manuscript.

Acknowledgments

The authors are grateful to the funding support from National Natural Science Foundation of China (31800806, 31872748, 81925027, 31400826, 82072424), Jiangsu Provincial Special Program of Medical Science (BL2012004), Applied Basic Research Project of Changzhou (CJ20180063), the Priority Academic Program Development (PAPD) of Jiangsu Higher Education Institutions, and Young Talent Development Plan of Changzhou Health Commission (CZQM2020003). RHM and WS acknowledge the funding support from the EPSRC (Funding Reference Number EP/L015995/1).

References

[1] G.M. Crane, S.L. Ishaug, A.G. Mikos. Bone tissue engineering. Nat. Med. 1 (12) (1995) 1322.
[2] G.J. Meijer, J.D. de Bruijn, R. Koole, C.A. van Blitterswijk. Cell based bone tissue engineering in jaw defects. Biomaterials 29 (21) (2008) 3053-3061.
[3] P.J. Stiers, G.N. Van, G. Carmeliet. Targeting the hypoxic response in bone tissue engineering: A balance between supply and consumption to improve bone regeneration. Mo. Cell. Endocrinol. 432 (C) (2016) 96-105.
[4] C. Liang, B. Guo, H. Wu, N. Shao, D. Li, J. Liu, L. Dang, C. Wang, H. Li, S. Li. Aptamer-functionalized lipid nanoparticles targeting osteoblasts as a novel RNA interference-based bone anabolic strategy. Nat. Med. 21 (3) (2015) 288.
[5] Y. Peck, P. He, G.S.V. Chilla, C.L. Poh, D.-A. Wang. A preclinical evaluation of an autologous living hyaline-like cartilaginous graft for articular cartilage repair: a pilot study. Sci. Rep. 5 (2015) 16225.
[6] R.K. Das, V. Gocheva, R. Hammink, O.F. Zouani, A.E. Rowan. Stress-stiffening-mediated stem-cell commitment switch in soft responsive hydrogels. Nat. Mater. 15 (3) (2016) 318-325.
[7] X. Liu, X. Jin, P.X. Ma. Nanofibrous hollow microspheres self-assembled from star-shaped polymers as injectable cell carriers for knee repair. Nat. Mater. 10 (5) (2011) 398-406.
[8] N. Koike, D. Fukumura, O. Gralla, P. Au, J.S. Schechner, R.K. Jain. Tissue engineering: creation of long-lasting blood vessels. Nature 428 (6979) (2004) 138-139.
[9] J.M. Karp, G.S.L. Teo. Mesenchymal Stem Cell Homing: The Devil Is in the Details. Cell Stem Cell 4 (3) (2009) 206-216.
[10] M. Honczarenko, Y. Le, M. Swierkowski, I. Ghiran, A.M. Glodek, L.E. Silberstein. Human bone marrow stromal cells express a distinct set of biologically functional chemokine receptors. Stem Cells 24 (4) (2006) 1030-1041.
[11] X. Hu, Y. Wang, Y. Tan, J. Wang, H. Liu, Y. Wang, S. Yang, M. Shi, S. Zhao, Y. Zhang, Q. Yuan. A Difunctional Regeneration Scaffold for Knee Repair based on Aptamer-Directed Cell Recruitment. Adv. Mater. 29 (15) (2017) 1605235.
[12] K.I. Kap, L.S. Jin, A. Anthony, J.J. Yoo. In situtissue regeneration through host stem cell recruitment. Exp. Mol. Med. 45 (11) (2013) e57.
[13] L.L. Hench, I.D. Xynos, J.M. Polak. Bioactive glasses for in situ tissue regeneration. J. Biomater. Sci.-Polym. Ed. 15 (4) (2004) 543-562.
[14] E. Anitua, M. Sanchez, G. Orive. Potential of endogenous regenerative technology for in situ regenerative medicine. Adv. Drug. Deliv. Rev. 62 (7-8) (2010) 741-752.
[15] M. Ullah, D.D. Liu, A.S. Thakor. Mesenchymal Stromal Cell Homing: Mechanisms and Strategies for Improvement. iScience 15 (2019) 421-438.
[16] J.E. Won, Y.S. Lee, J.H. Park, J.H. Lee, Y.S. Shin, C.H. Kim, J.C. Knowles, H.W. Kim. Hierarchical microchanneled scaffolds modulate multiple tissue-regenerative processes of immune-responses, angiogenesis, and stem cell homing. Biomaterials 227 (2020) 119548.
[17] Y. Shi, R. He, X. Deng, Z. Shao, D. Deganello, C. Yan, X. Z. Three-dimensional biofabrication of an aragonite-enriched self-hardening bone graft substitute and assessment of its osteogenicity in vitro and in vivo. Biomaterials Translational 1 (1) (2020) 69-81.

[18] J. Yuan, P. Maturavongsadit, Z. Zhou, B. Lv, Y. Lin, J. Yang, J.A. Luckanagul. Hyaluronic acid-based hydrogels with tobacco mosaic virus containing cell adhesive peptide induce bone repair in normal and osteoporotic rats. Biomaterials Translational 1 (1) (2020) 89-98.
[19] J.T. Triffitt. Orthopaedic tissue engineering and stem cells - an unfulfilled promise. Biomaterials Translational 2 (2021) 0-0.
[20] R. Wu, X. Xu, J. Wang, X. He, H. Sun, F. Chen. Biomaterials for endogenous regenerative medicine: coaxing stem cell homing and beyond. Appl. Mater. Today. 11 (2018) 144-165.
[21] D. Orlic, J. Kajstura, S. Chimenti, I. Jakoniuk, S.M. Anderson, B. Li, J. Pickel, R. McKay, B. Nadal-Ginard, D.M. Bodine. Bone marrow cells regenerate infarcted myocardium. Nature 410 (6829) (2001) 701.
[22] M. Dominici, B.K. Le, I. Mueller, I. Slapercortenbach, F. Marini, D. Krause, R. Deans, A. Keating, P. Dj, E. Horwitz. Minimal criteria for defining multipotent mesenchymal stromal cells. The International Society for Cellular Therapy position statement. Cytotherapy 8 (4) (2006) 315.
[23] C.H. Kim, H.E. Broxmeyer. In vitro behavior of hematopoietic progenitor cells under the influence of chemoattractants: stromal cell-derived factor-1, steel factor, and the bone marrow environment. Blood 91 (1) (1998) 100-110.
[24] G. Forte, M. Minieri, P. Cossa, D. Antenucci, M. Sala, V. Gnocchi, R. Fiaccavento, F. Carotenuto, P. De Vito, P.M. Baldini, M. Prat, P. Di Nardo. Hepatocyte growth factor effects on mesenchymal stem cells: proliferation, migration, and differentiation. Stem Cells 24 (1) (2006) 23-33.
[25] S. Neuss, E. Becher, M. Wöltje, L. Tietze, W. Jahnen-Dechent. Functional expression of HGF and HGF receptor/c-met in adult human mesenchymal stem cells suggests a role in cell mobilization, tissue repair, and wound healing. Stem Cells 22 (3) (2010) 405-414.
[26] N. Quirici, D. Soligo, P. Bossolasco, F. Servida, C. Lumini, G.L. Deliliers. Isolation of bone marrow mesenchymal stem cells by anti-nerve growth factor receptor antibodies. Exp. Hematol. 30 (7) (2002) 783-791.
[27] R.J. Cuthbert, P.V. Giannoudis, X.N. Wang, L. Nicholson, D. Pawson, A. Lubenko, H.B. Tan, A. Dickinson, D. Mcgonagle, E. Jones. Examining the feasibility of clinical grade CD271+ enrichment of mesenchymal stromal cells for bone regeneration. Plos One 10 (3) (2015) e0117855.
[28] S. Kuci, Z. Kuci, H. Kreyenberg, E. Deak, K. Putsch, S. Huenecke, C. Amara, S. Koller, E. Rettinger, M. Grez, U. Koehl, H. Latifi-Pupovci, R. Henschler, T. Tonn, D. von Laer, T. Klingebiel, P. Bader. CD271 antigen defines a subset of multipotent stromal cells with immunosuppressive and lymphohematopoietic engraftment-promoting properties. Haematologica 95 (4) (2010) 651-659.
[29] H.J. Bühring, V.L. Battula, S. Treml, B. Schewe, L. Kanz, W. Vogel. Novel markers for the prospective isolation of human MSC. Ann. NY. Acad. Sci. 1106 (1) (2007) 262.
[30] S.A. Boxall, E. Jones. Markers for characterization of bone marrow multipotential stromal cells. Stem. Cells. Int. 2012 (2012) 975871.
[31] E.S. Anton, G. Weskamp, L.F. Reichardt, W.D. Matthew. Nerve growth factor and its low-affinity receptor promote Schwann cell migration. Proc. Natl. Acad. Sci. U S A. 91 (7) (1994) 2795-2799.
[32] Y. Jiang, C. Hu, S. Yu, J. Yan, H. Peng, H.W. Ouyang, R.S. Tuan. Cartilage stem/progenitor cells are activated in osteoarthritis via interleukin-1β/nerve growth factor signaling. Arthritis. Res. Ther. 17 (2015) 327.
[33] P. Bianco, X. Cao, P.S. Frenette, J.J. Mao, P.G. Robey, P.J. Simmons, C.Y. Wang. The meaning,

the sense and the significance: translating the science of mesenchymal stem cells into medicine. Nat. Mater. 19 (1) (2013) 35.
[34] J.T. Watson, T. Foo, J. Wu, B.R. Moed, M. Thorpe, L. Schon, Z. Zhang. CD271 as a marker for mesenchymal stem cells in bone marrow versus umbilical cord blood. Cells Tissues Organs 197 (6) (2013) 496-504.
[35] C.A. Custodio, M.T. Cerqueira, A.P. Marques, R.L. Reis, J.F. Mano. Cell selective chitosan microparticles as injectable cell carriers for tissue regeneration. Biomaterials 43 (2015) 23-31.
[36] T. Gao, N. Zhang, Z. Wang, Y. Wang, Y. Liu, Y. Ito, P. Zhang. Biodegradable Microcarriers of Poly(Lactide-co-Glycolide) and Nano-Hydroxyapatite Decorated with IGF-1 via Polydopamine Coating for Enhancing Cell Proliferation and Osteogenic Differentiation. Macromol Biosci 15 (8) (2015) 1070-1080.
[37] A. Kumachev, J. Greener, E. Tumarkin, E. Eiser, P.W. Zandstra, E. Kumacheva. High-throughput generation of hydrogel microbeads with varying elasticity for cell encapsulation. Biomaterials 32 (6) (2011) 1477-1483.
[38] B.P. Chan, T.Y. Hui, M.Y. Wong, K.H. Yip, G.C. Chan. Mesenchymal stem cell-encapsulated collagen microspheres for bone tissue engineering. Tissue Eng Part C Methods 16 (2) (2010) 225-235.
[39] A. Moshaverinia, X. Xu, C. Chen, K. Akiyama, M.L. Snead, S. Shi. Dental mesenchymal stem cells encapsulated in an alginate hydrogel co-delivery microencapsulation system for cartilage regeneration. Acta Biomater 9 (12) (2013) 9343-9350.
[40] H. Lee, S.M. Dellatore, W.M. Miller, P.B. Messersmith. Mussel-inspired surface chemistry for multifunctional coatings. Science 318 (5849) (2007) 426-430.
[41] J. Yan, L. Yang, M.F. Lin, J. Ma, X. Lu, P.S. Lee. Polydopamine spheres as active templates for convenient synthesis of various nanostructures. Small 9 (4) (2013) 596-603.
[42] C. Wu, P. Han, X. Liu, M. Xu, T. Tian, J. Chang, Y. Xiao. Mussel-inspired bioceramics with self-assembled Ca-P/polydopamine composite nanolayer: preparation, formation mechanism, improved cellular bioactivity and osteogenic differentiation of bone marrow stromal cells. Acta. Biomater. 10 (1) (2014) 428-438.
[43] H. Zhao, J. Feng, T.V. Ho, W. Grimes, M. Urata, Y. Chai. The suture provides a niche for mesenchymal stem cells of craniofacial bones. Nat. Cell. Biol. 17 (4) (2015) 386-396.
[44] H. Zhao, J. Feng, K. Seidel, S. Shi, O. Klein, P. Sharpe, Y. Chai. Secretion of shh by a neurovascular bundle niche supports mesenchymal stem cell homeostasis in the adult mouse incisor. Cell Stem Cell 14 (2) (2014) 160.
[45] W. Lin, L. Xu, S. Zwingenberger, E. Gibon, S.B. Goodman, G. Li. Mesenchymal stem cells homing to improve bone healing. J. Orthop. Translat. 9 (2017) 19-27.
[46] Y. Shi, G. He, W.C. Lee, J.A. McKenzie, M.J. Silva, F. Long. Gli1 identifies osteogenic progenitors for bone formation and fracture repair. Nat. Commun. 8 (1) (2017) 2043.
[47] M. González, L.A. Bagatolli, I. Echabe, J.L. Arrondo, C.E. Argaraña, C.R. Cantor, G.D. Fidelio. Interaction of biotin with streptavidin. Thermostability and conformational changes upon binding. J. Biol. Chem. 272 (17) (1997) 11288.
[48] L.M. Schäck, S. Noack, R. Weist, M. Jagodzinski, C. Krettek, M. Buettner, A. Hoffmann. Analysis of surface protein expression in human bone marrow stromal cells: new aspects of culture-induced changes, inter-donor differences and intracellular expression. Stem Cells Dev 22 (24) (2013) 3226-3235.

[49] E. Flores-Torales, A. Orozco-Barocio, O.R. Gonzalez-Ramella, A. Carrasco-Yalan, K. Gazarian, S. Cuneo-Pareto. The CD271 expression could be alone for establisher phenotypic marker in Bone Marrow derived mesenchymal stem cells. Folia Histochem Cytobiol 48 (4) (2010) 682-686.
[50] N. Quirici, C. Scavullo, L. de Girolamo, S. Lopa, E. Arrigoni, G.L. Deliliers, A.T. Brini. Anti-L-NGFR and -CD34 monoclonal antibodies identify multipotent mesenchymal stem cells in human adipose tissue. Stem Cells Dev 19 (6) (2010) 915-925.
[51] M. Álvarez-Viejo, Y. Menéndez-Menéndez, J. Otero-Hernández. CD271 as a marker to identify mesenchymal stem cells from diverse sources before culture. World J Stem Cells 7 (2) (2015) 470-476.
[52] C. Wu, Y. Zhang, Y. Zhou, W. Fan, Y. Xiao. A comparative study of mesoporous glass/silk and non-mesoporous glass/silk scaffolds: physiochemistry and in vivo osteogenesis. Acta. Biomater. 7 (5) (2011) 2229-2236.
[53] Y. Liu, K. Ai, L. Lu. Polydopamine and its derivative materials: synthesis and promising applications in energy, environmental, and biomedical fields. Chem. Rev. 114 (9) (2014) 5057-5115.
[54] W.B. Tsai, W.T. Chen, H.W. Chien, W.H. Kuo, M.J. Wang. Poly(dopamine) coating of scaffolds for articular cartilage tissue engineering. Acta. Biomater. 7 (12) (2011) 4187-4194.
[55] Z. Liu, S. Qu, X. Zheng, X. Xiong, R. Fu, K. Tang, Z. Zhong, J. Weng. Effect of polydopamine on the biomimetic mineralization of mussel-inspired calcium phosphate cement in vitro. Mater. Sci. Eng. C. Mater. Biol. Appl. 44 (2014) 44-51.
[56] M. Ventura, Y. Sun, S. Cremers, P. Borm, Z.T. Birgani, P. Habibovic, A. Heerschap, P.M. van der Kraan, J.A. Jansen, X.F. Walboomers. A theranostic agent to enhance osteogenic and magnetic resonance imaging properties of calcium phosphate cements. Biomaterials 35 (7) (2014) 2227-2233.
[57] C. Shi, Z. Yuan, F. Han, C. Zhu, B. Li. Polymeric biomaterials for bone regeneration. Ann. Jt. 1 (2016) 27.
[58] F.P. Barry, J.M. Murphy. Mesenchymal stem cells: clinical applications and biological characterization. Int. J. Biochem. Cell. Biol. 36 (4) (2004) 568-584.

Supporting Information

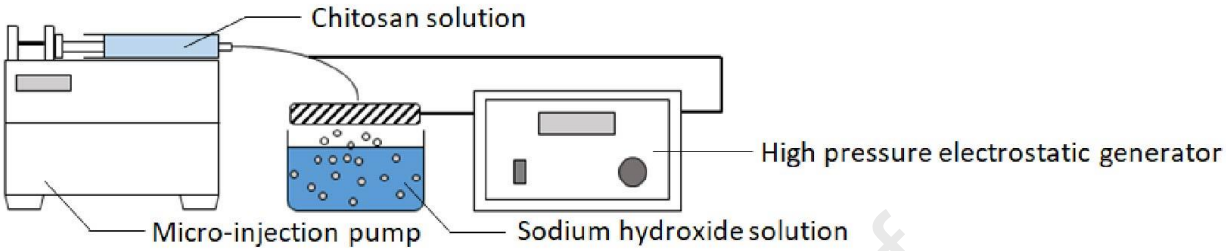

Fig. S1. Illustration of the setup used for preparing chitosan microspheres.

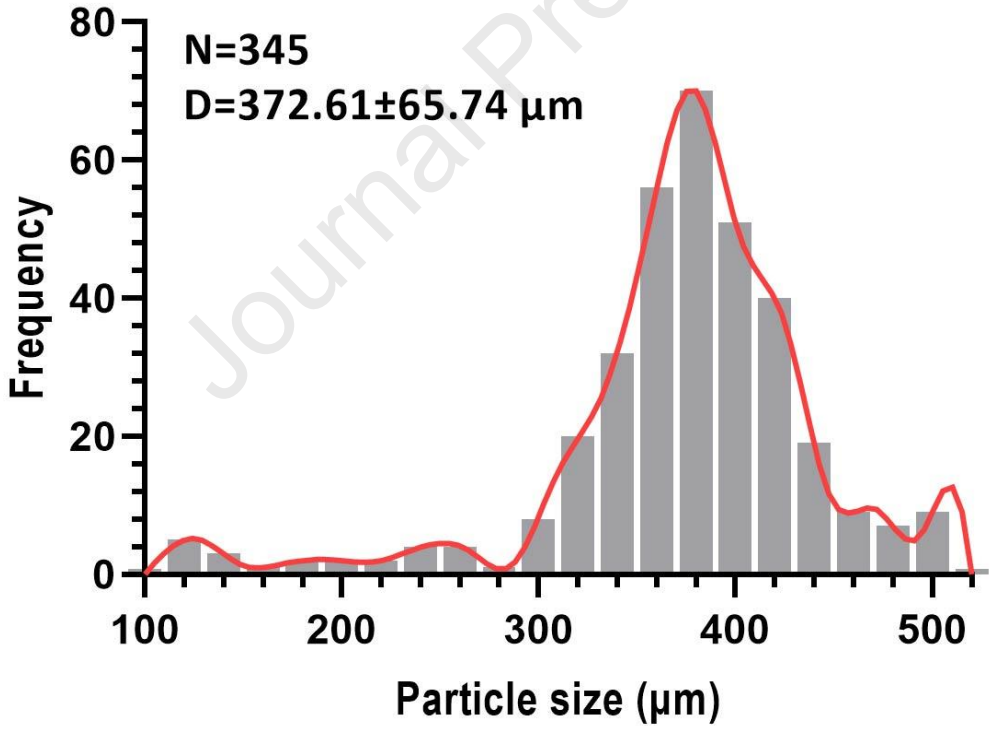

Fig. S2. Histogram of the distribution of microparticle size.

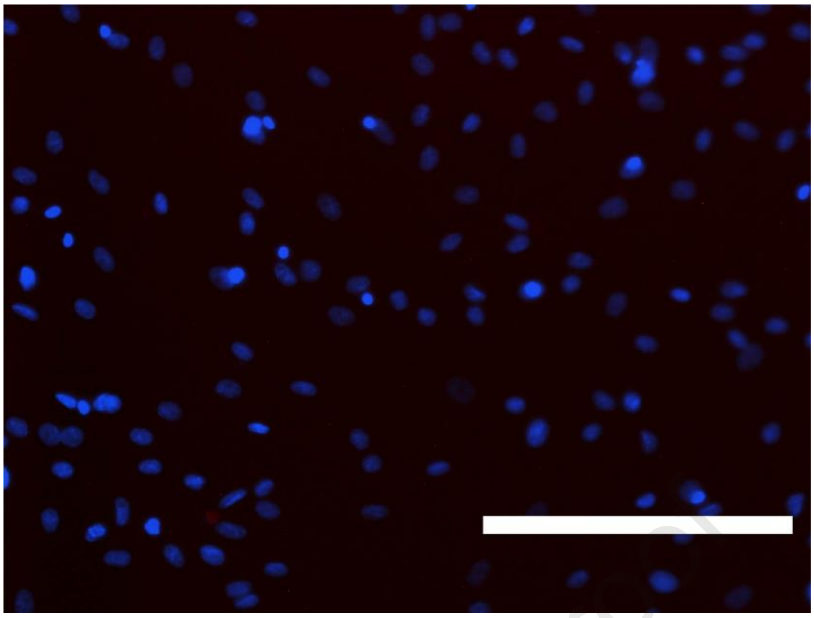

Fig. S3. Immunofluorescence assays of hBM-MSCs stained by PE-CD34 antibody as negative control. Scale bar, 200 μm.

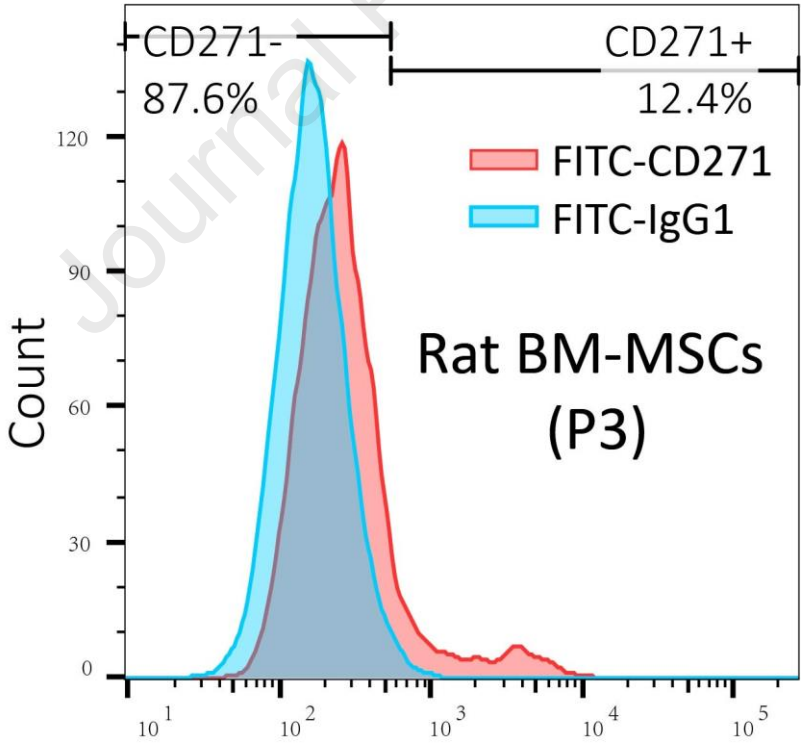

Fig. S4. Flow cytometry of rat BM-MSCs (P3).

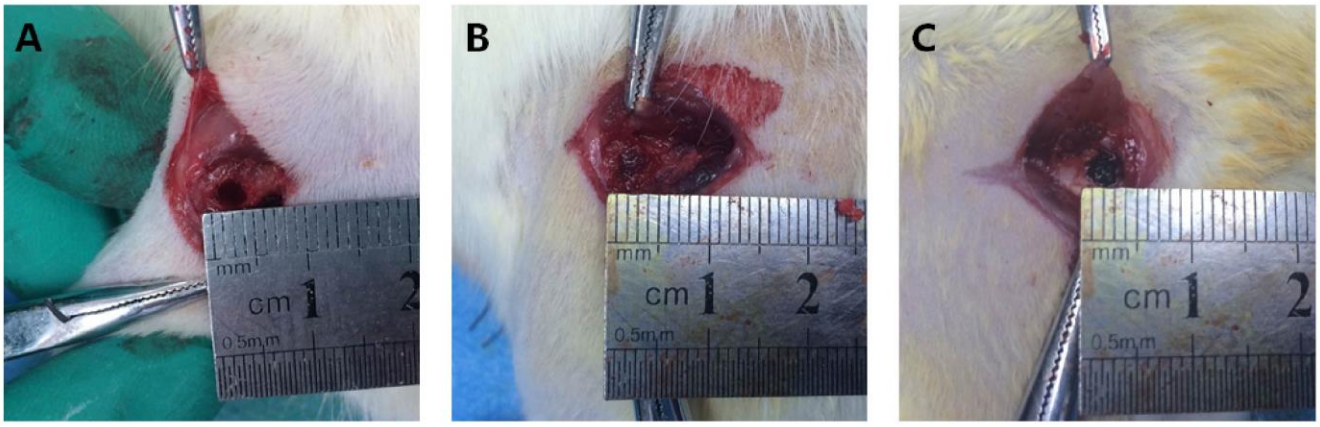

Fig. S5. Bone defect of femoral condyle (A) and after implantation of CD271/CS (B) or CD271/PDA/CS microspheres (C).

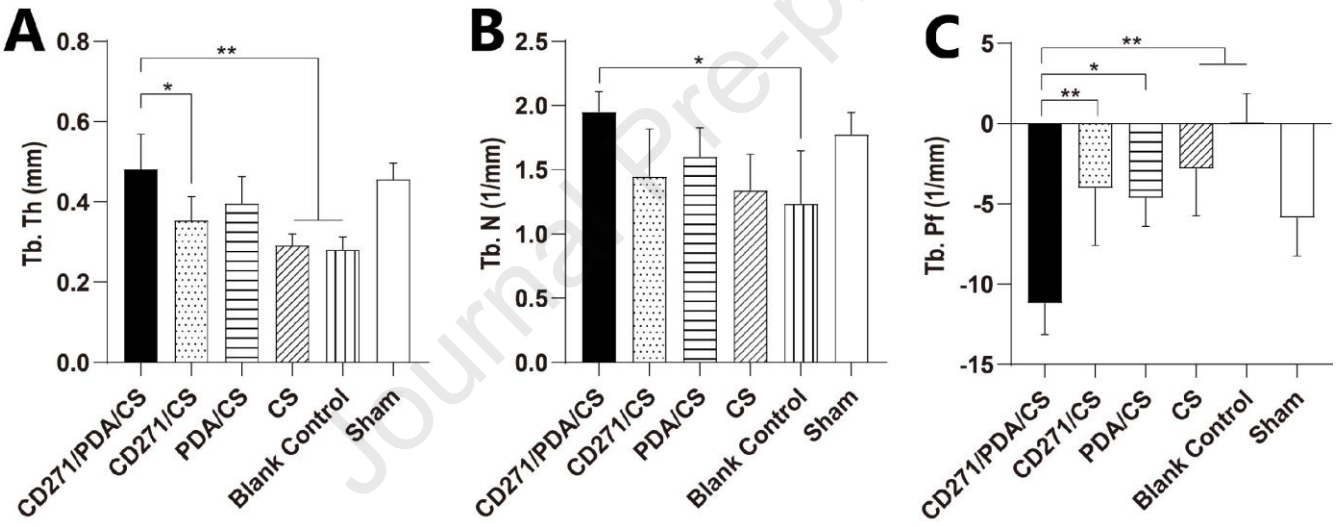

Fig. S6. Analysis of trabecular bone related results at 12 weeks postoperatively. (A) Results of trabecular thickness (Tb. Th). (B) Results of trabecular number (Tb. N). (C) Results of trabecular pattern factor (Tb. Pf). * $p < 0.05$ and ** $p < 0.01$.

Table S1. The characteristics of SD rats in animal surgeries.

	CD271/PDA/CS	CD271/CS	PDA/CS	CS	Blank control	Sham
Characteristics						
Age (weeks)	8.5	8.5	8.5	8.5	8.5	8.5
Sex	Male	Male	Male	Male	Male	Male
Weight (g)	252.87±5.85	251.53±7.02	247.94±4.80	248.93±7.10	250.29±7.34	248.86±6.31
Sample Size						
3 days	4	4	4	4	0	0
7 days	4	4	4	4	0	0
6 weeks	4	4	4	4	4	4
12 weeks	4	4	4	4	4	4
Loss	0	0	0	0	0	0

Declaration of interests

☒The authors declare that they have no known competing financial interests or personal relationships that could have appeared to influence the work reported in this paper.

☐The authors declare the following financial interests/personal relationships which may be considered as potential competing interests: